Chapter 8

Quantitative DWI implemented after DCE-MRI yields increased specificity for BI-RADS 3 and 4 breast lesions

Hildebrand Dijkstra
Monique D. Dorrius
Mirjam Wielema
Ruud M. Pijnappel
Matthijs Oudkerk
Paul E. Sijens

Published in the Journal of Magnetic Resonance Imaging
2016, doi 10.1002/jmri.25331.

8.1 Abstract

Purpose: To assess if specificity can be increased when semi-automated breast lesion analysis of quantitative diffusion-weighted imaging (DWI) is implemented after dynamic contrast-enhanced (DCE-) MRI in the workup of BI-RADS 3 and 4 breast lesions larger than 1 cm.

Materials and Methods: 120 consecutive patients (mean age, 48 years; age range, 23–75 years) with 139 breast lesions (≥1cm) were examined (2010—2014) with 1.5T DCE-MRI and DWI (b=0, 50, 200, 500, 800 and 1000 s/mm^2) and the BI-RADS classification and histopathology were obtained. For each lesion malignancy was excluded using voxelwise semi-automated breast lesion analysis based on previously defined thresholds for the apparent diffusion coefficient (ADC) and the three intravoxel incoherent motion (IVIM) parameters: molecular diffusion (D_{slow}), microperfusion (D_{fast}), and the fraction of D_{fast} (f_{fast}). The sensitivity (Se), specificity (Sp) and negative-predictive-value (NPV) based on only IVIM parameters combined in parallel (D_{slow}, D_{fast} and f_{fast}), or the ADC or the BI-RADS classification by DCE-MRI were compared. Subsequently, the Se, Sp and NPV of the combination of the BI-RADS classification by DCE-MRI followed by the IVIM parameters in parallel (or the ADC) were compared.

Results: Twenty-three of 139 breast lesions were benign. Se and Sp of DCE-MRI were 100% and 30.4% (NPV=100%). Se and Sp of IVIM parameters in parallel were 92.2% and 52.2% (NPV=57.1%) and for the ADC 95.7% and 17.4%, respectively (NPV=44.4%). 26 of 139 lesions were classified as BI-RADS 3 (n=7) or BI-RADS 4 (n=19). DCE-MRI combined with ADC (Se=99.1%, Sp=34.8%) or IVIM (Se=99.1%, Sp=56.5%) did significantly improve (p=0.016) Sp of DCE-MRI alone for workup of BI-RADS 3 and 4 lesions (NPV=92.9%).

Conclusion: Quantitative DWI has a lower NPV compared to DCE-MRI for evaluation of breast lesions and may therefore not be able to replace DCE-MRI; when implemented after DCE-MRI as problem solver for BI-RADS 3 and 4 lesions the combined specificity improves significantly.

8.2 Introduction

Diffusion-weighted imaging (DWI) is currently not generally implemented in the diagnostic workup of breast pathology. After the combination of mammography and ultrasound, dynamic contrast-enhanced (DCE-) MRI is the second most used modality. DCE-MRI has the highest overall negative predictive value (NPV) of all imaging techniques, and is usually able to safely exclude malignancy (NPV > 98%) (*1–4*). However, enhancement patterns of benign and malignant breast lesions can show considerable overlap on DCE-MRI, especially for BI-RADS 3 and 4 lesions (*1, 3, 4*). For those breast lesions it is often unclear if the lesion is a cancer based on only the enhancement curve, for example a fibro adenoma often appears as malignant due to late wash-out of the kinetic curve. In clinical practice the majority of patients with these difficult to differentiate breast lesions on DCE-MRI will undergo a biopsy with its known complications (*5*). At this point in the diagnostic algorithm, quantitative DWI might have the potential to be implemented for excluding malignancy in this group of equivocal breast lesions on DCE-MRI (*6*).

DWI of breast lesions can be quantified using a mono-exponential model yielding the apparent diffusion coefficient (ADC) or a bi-exponential model such as intravoxel incoherent motion (IVIM) (*7*). The ADC has been shown already to be a valuable noninvasive quantitative biomarker to assess breast cancer (*8*). Also IVIM has the potential to provide additional diagnostic performance and proves generally a higher specificity for breast cancer compared to the ADC (*9–11*).

In a preceding optimization and validation study, IVIM and ADC were optimized for excluding malignancy of breast lesions using semi-automated breast lesion analysis (*12*). The included lesions were larger than 1 cm to allow for optimal voxelwise analysis using DWI, which has generally a relatively low spatial resolution. The effect of lesion size on the NPV was suspected to be minimal; the NPV of the ADC has been reported similar (96%) for small (≤ 1 cm) and large (> 1 cm) lesions (*13*). The statistics will be affected though by the high percentage of malignancy (66.7-95.9%) when only large lesions are included (*14, 15*).

The potential value of combined quantitative DWI and DCE-MRI for breast lesion differentiation has been indicated already, but is generally based on the ADC, and the selection of the region-of-interest usually relies on drawing a circular area and taking the average (*16–18*). Additionally, for DWI to be implemented successfully along DCE-MRI, the sensitivity should be high (>98%) while the specificity is maximized. These opportunities were implemented in a method defined as semi-automated breast lesion

analysis and is described in the previous study (*12*).

This prior article dealt with the optimization and validation of IVIM compared with the ADC for the semi-automated analysis of breast lesions using a multi-reader setup, which requires the definition of a freeform margin around the lesion resulting in automated inclusion of a selection of voxels within it, thereby maximizing specificity while aiming for a sensitivity near 100%. In the current manuscript we apply the previously validated and optimized semi-automated breast lesion analysis by implementing it after DCE-MRI.

The purpose of this study was therefore to assess if specificity can be increased when semi-automated breast lesion analysis of quantitative DWI is implemented after DCE-MRI in the workup of BI-RADS 3 and 4 breast lesions larger than 1 cm.

8.3 Materials and methods

8.3.1 Study population

The protocol of this prospective study was approved by the hospital's institutional review board and all patients provided informed consent. Between May 2010 and July 2014, patients with an inconclusive mammogram or part of the BRCA screening population and scheduled for breast MRI and DWI were recruited. Inclusion criteria were: lesion diameter larger than or equal to 1 cm on MRI, no hematomas, pathology available, and no previous breast surgery or breast implants. This resulted in the inclusion of 120 consecutive patients (mean age, 48 years; age range, 23–75 years) with 139 breast lesions: 116 malignant and 23 benign. All 120 patients have been previously reported (*12*).

8.3.2 Pathology

Histopathology, cytology or at least 6 months follow-up of the 139 breast lesions defined lesions as benign or malignant. Tissue samples were obtained after modified radical mastectomy (n = 75), lumpectomy (n = 39), ultrasonographically (US) guided core biopsy (n = 16), US-guided fine-needle aspiration biopsy (n = 3) and MRI-guided core biopsy (n = 1). Five lesions were negative during MRI follow-up (mean follow-up time: 1.5 years; mean follow-up frequency: 11 months).

8.3.3 MR protocols

All subjects were examined on a 1.5T MRI system (Magnetom Avanto, Siemens Medical Solutions, Erlangen, Germany). The body coil served as transmitter and a commercially available circularly polarized bilateral breast phased-array coil with automatic tuning and electronic decoupling as receiver (Siemens Medical Solutions). After the localizer scans, DWI was performed using a spin echo based single shot echo-planar imaging (SS-EPI) sequence in combination with spectral adiabatic inversion recovery (SPAIR) fat suppression. DWI acquisitions (b = 0, 50, 200, 500, 800 and 1000 s/mm^2) were tuned with the following parameters: TR 9300 ms; TE 91 ms; FA 90°; slice-thickness 4 mm; slice-gap 6 mm; FOV 170 × 340 mm^2; matrix 192 × 384; bandwidth 1628 Hz/pixel; 2 averages. Diffusion gradients (25 mT/m) were applied in the phase-, read-, and z-directions separately. In total, 28 transverse slices were acquired in interleaved mode to cover both breasts within an acquisition time of 2.5 minutes.

Finally, eight series (six series from July 2013) of transversal DCE T1-weighted spoiled gradient echo sequences were obtained with a temporal resolution of 76 seconds using gadoterate meglumine (Gd-DOTA, Dotarem, Guerbet, 0.1 mmol/kg): TR 4.17 ms; TE 1.29 ms; FA 10°; slice-thickness 0.97 mm; no slice-gap; FOV 340 × 340 mm^2; matrix 384 × 384; bandwidth 318 Hz/pixel; no averages. Parallel acquisition technique GRAPPA with acceleration factor 2 was enabled in all acquisitions.

8.3.4 DWI analysis

All 139 lesions were analyzed off-line (Matlab 2014a, The Mathworks, Natick, MA, USA) by a radiologist (R.M.P.) with 25 years of experience in mammography using the semi-automated method as described in the preceding optimization and validation study (*12*). For all lesions, the radiologist included voxels by drawing a freeform region-of-interest (ROI) around the lesion. The voxels included in the ROI were then fitted using both the bi-exponential IVIM model and a mono-exponential model using all 6 b-values yielding the ADC.

For the IVIM model the diffusion-weighted signal intensities S were fitted as follows (*7*, *19*):

$$\frac{S}{S_0} = f_{fast} \cdot \mathrm{e}^{-b \cdot D_{fast}} + f_{slow} \cdot \mathrm{e}^{-b \cdot D_{slow}} \tag{8.1}$$

where S_o is the maximum signal intensity, D_{fast} is the fast component representing microperfusion, f_{fast} is the fraction of microperfusion, D_{slow} is the slow component representing molecular diffusion and f_{slow} is the fraction of molecular diffusion ($f_{slow} = 1 - f_{fast}$).

Equation 8.1 was fitted by the Nelder-Mead simplex direct search method with bound constraints, which performs a constrained non-linear minimisation of the sum of the squared residuals (*20*, *21*). The initial guess D^o_{slow} was estimated by calculating the slope of the asymptote of the slow signal component between b = 500 and 1000 s/mm², and D_{slow} was bound between $0.2 \times D^o_{slow} \times 10^{-3}$ mm²/s and $5 \times D^o_{slow} \times 10^{-3}$ mm²/s. The slope of the signal between b = 0 and b = 50 s/mm² was used to guess the initial value of the microperfusion (D^o_{fast}), and was bound between D^o_{slow} and 100×10^{-3} mm²/s. The initial guess of f_{fast} (f^o_{fast}) was estimated simply by solving equation 8.1 for f_{fast} as all other parameters are known and $f_{slow} = 1 - f_{fast}$, and no restrictions were applicable (bound between 0.0 and 1.0).

Subsequently, the voxels within the ROI were automatically processed off-line according to the two previously determined optimized parameters as described in the preceding optimization and validation study (*12*): optimal fraction (Fo) and thresholds (TH). The Fo defined which voxels of the lesions were used based on the magnitude of D_{slow}, D_{fast} and f_{fast} (and similar for ADC as well), and were respectively 61%, 85%, 100% and 100%. This means that for instance for D_{slow}, only the 61% lowest D_{slow} voxels in the lesion are used to calculate the median D_{slow} of the lesion. The optimized TH were 1.44×10^{-3} mm²/s, 18.55×10^{-3} mm²/s and 0.247 for D_{slow}, D_{fast} and f_{fast} respectively.

The sensitivity (Se), specificity (Sp) and negative-predictive-value (NPV) resulted from combining the three IVIM parameters in parallel in a single test using the "AND rule" to discriminate malignant from benign lesions, based on the TH resulting from the preceding optimization and validation study. That is, if D_{slow} was lower than the TH, and if D_{fast} was lower than the TH, and if f_{fast} was lower than the TH, then the combined result was defined positive (malignant), but in all other cases, the combined result was negative (benign). For the ADC one TH was applied (2.00×10^{-3} mm²/s) and the result was defined malignant if ADC was lower than the TH.

8.3.5 DCE-MRI analysis

All patients' images were clinically interpreted by two radiologists with 3 and 30 years of experience in mammography and the findings were recorded in structured ra-

diology reports. The Breast Imaging-Reporting and Data System (BI-RADS) classification was extracted retrospectively from the structured radiology reports for all 139 lesions. Lesions which MRI classified as BI-RADS 1 or 2 were considered negative for malignancy. Next, Se, Sp and NPV were calculated.

8.3.6 Statistics

Statistical analyses were performed using SPSS (SPSS 22, Chicago, IL, USA). All data were tested for normality using Shapiro–Wilk tests. IVIM parameters and ADC were given as median. The diagnostic performance in terms of Se, Sp and NPV was compared between DWI (IVIM and ADC) and DCE-MRI (BI-RADS classification) using McNemar's test based on the binomial distribution. In addition, the combinations of IVIM or ADC following DCE-MRI were compared.

For Se and Sp, the 95% confidence intervals (CI) for proportions were calculated according to the efficient-score method (corrected for continuity) described by Newcombe et al. (*22*). For all statistical tests $P < 0.05$ was considered to indicate a statistically significant difference.

8.4 Results

8.4.1 Comparison of DCE-MRI and quantitative DWI as individual techniques

All 139 breast lesions exceeding 1 cm on DCE-MRI were classified according to the BI-RADS classification: BI-RADS 2 (n = 7), BI-RADS 3 (n = 7), BI-RADS 4 (n = 19), BI-RADS 5 (n = 73) and BI-RADS 6 (n = 33). One hundred sixteen out of 139 breast lesions (83.5%) were proven malignant by pathology.

After reviewing all 139 lesions, the overall Se and Sp of DCE-MRI were 100% and 30.4% respectively when lesions classified as BI-RADS ≥ 3 were considered malignant (Table 8.1). Using DCE-MRI, 7 out of 23 benign lesions were true negatives (TN) that could be safely excluded from further diagnostic workup (BI-RADS 2), and there were no false negatives (NPV = 100%). The overall NPV of DWI using IVIM was 57.1% with a Se of 92.2% and Sp of 52.2% (significantly different from DCE-MRI, p = 0.003), and as many as 12 benign lesions would have been excluded from further diagnostic workup;

at the same time there would have been 9 false negatives. The overall NPV of the ADC was 44.4% with a Se of 95.7% and Sp of 17.4%, and based on the ADC alone, only 4 benign lesions would have been excluded from further diagnostic workup while there were 5 false negatives.

When only BI-RADS 3 and 4 lesions were considered, the NPV was 50.0% and 85.7% respectively for the ADC and IVIM individually.

Table 8.1: Comparison of the diagnostic performance of DCE-MRI and quantitative DWI as individual techniques. Demonstrated is the diagnostic performance and 95% CI to exclude breast cancer compared between DCE-MRI, IVIM and ADC as individual techniques. Data are provided for all lesions (n = 139) and also for BI-RADS 3 and 4 lesions only (n = 26). Quantitative DWI has a lower NPV compared to DCE-MRI for evaluation of breast lesions and may therefore not be able to replace DCE-MRI. * indicates a significant difference.

	TP	TN	FP	FN	Se (%)	Sp (%)	NPV (%)	
all lesions (n = 139)								
DCE-MRI	116	7	16	0	100 (96.0-100)	30.4 (14.0-53.0)	100 (56.0-100)	
ADC	111	4	19	5	95.7 (89.7-98.4)	17.4 (0.06-39.5)	44.4 (15.3-77.3)	p = 0.77 vs. DCE-MRI
IVIM	107	12	11	9	92.2 (85.4-96.2)	52.2 (31.1-72.6)	57.1 (34.4-77.4)	p = 0.003* vs. DCE-MRI
BI-RADS 3 and 4 lesions (n = 26)								
ADC	14	1	10	1	93.3 (66.0-99.7)	9.1 (0.0-42.9)	50.0 (2.6-97.3)	
IVIM	14	6	5	1	93.3 (66.0-99.7)	54.5 (24.6-81.9)	85.7 (42.0-99.2)	

8.4.2 Quantitative DWI following DCE-MRI as problem solver for BI-RADS 3 and 4 lesions

Pathology proved 11 out of 26 BI-RADS 3 and 4 lesions as benign (Fig. 8.1, Table 8.2). The overall Sp increased significantly (p = 0.016) from 30.4% (DCE-MRI only) to 56.5% (DCE-MRI + IVIM) with a NPV of 92.9%, when IVIM followed DCE-MRI as problem solver for BI-RADS 3 and 4 lesions (Table 8.3). For the ADC the overall Sp showed little change from 30.4% to 34.8%. IVIM identified 6 out of 11 benign lesions correctly as negative (Table 8.2). One of those benign lesions was proven adenosis and the parametric maps (D_{slow}, D_{fast} and f_{fast}) of this lesion obtained using IVIM are shown

in Fig. 8.2 for illustrative purposes. The ADC identified 1 out of 11 benign lesions correctly as negative.

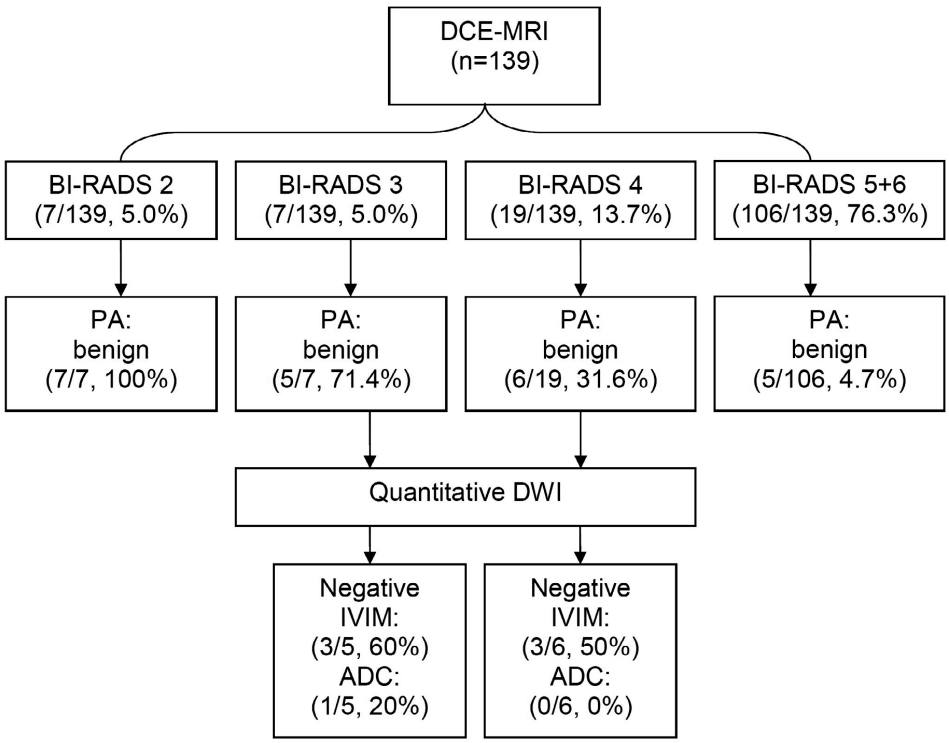

Figure 8.1: Flow chart of diagnostic workup. Lesions identified on DCE-MRI as BI-RADS 3 or 4 (n = 26) were additionally evaluated by quantitative DWI. For the remainder of the lesions (n = 113) the endpoint was DCE-MRI. DCE-MRI classified 11 benign lesions as BI-RADS 3 or 4; IVIM identified 6 of those lesions correctly as negative, for ADC this was 1 out of 11. This indicates the potential added value of DWI when implemented after DCE-MRI in the diagnostic workup of breast lesions, especially for BI-RADS 3 and 4 lesions.

Table 8.2: BI-RADS 3 and 4 lesions on DCE-MRI Listed are 26 lesions classified by DCE-MRI as inconclusive (BI-RADS 3 or 4). 11 out of 26 inconclusive lesions were proven benign by pathology, and IVIM identified 6 out of those 11 benign lesions correctly as negative. For the ADC this number was 1 out of 11 lesions.
† Lesion was defined as positive (malignant) if the apparent diffusion coefficient (ADC) < 2.00 $\times 10^{-3}$ mm^2/s, otherwise negative (benign).
‡ The three intravoxel incoherent motion (IVIM) parameters were combined in parallel in a single test using the "AND rule" to discriminate malignant from benign lesions, based on three thresholds. If molecular diffusion (D_{slow}), fraction of microperfusion (f_{fast}) and microperfusion (D_{fast}) were lower than their threshold (1.44 $\times 10^{-3}$ mm^2/s, 0.247 and 18.55 $\times 10^{-3}$ mm^2/s respectively) then the combined result was defined positive (malignant), but in all other cases, the combined result was negative (benign). Data are medians.
* Lesion is shown in Fig. 8.2

Pathology	BI-RADS DCE- MRI	ADC ($\times 10^{-3}$ mm^2/s)	ADC test †	D_{slow} ($\times 10^{-3}$ mm^2/s)	D_{fast} ($\times 10^{-3}$ mm^2/s)	f_{fast} (%)	3-para meter IVIM test ‡
Benign							
epithelial hyperplasia	3	1.32	+	0.64	6.09	0.18	+
fibroadenoma	3	2.27	-	1.86	0.00	0.00	-
	3	1.93	+	1.57	12.5	0.27	-
adenosis	3	1.77	+	1.56	7.62	0.15	- *
	4	1.25	+	1.05	4.47	0.08	+
	4	1.16	+	0.75	0.00	0.06	+
chronic inflammation	4	1.63	+	1.32	3.66	0.08	+
	4	1.78	+	1.61	0.00	0.06	-
	3	1.68	+	1.33	0.00	0.05	+
intraductal papilloma	4	1.92	+	1.61	0.00	0.00	-
fibrotic parenchyma	4	1.66	+	1.46	22.9	0.15	-

Malignant							
IDC	3	1.52	+	1.04	6.51	0.15	+
	3	1.44	+	1.08	4.59	0.08	+
	4	1.29	+	1.18	0.00	0.00	+
	4	0.93	+	0.58	3.97	0.15	+
	4	0.99	+	0.81	0.00	0.00	+
	4	2.00	-	1.71	0.00	0.00	-
IDC + DCIS grade 2	4	0.96	+	0.55	11.1	0.16	+
IDC + DCIS grade 1	4	1.70	+	1.11	5.31	0.10	+
DCIS grade 3	4	1.38	+	1.21	7.09	0.09	+
	4	1.11	+	0.80	6.12	0.18	+
invasive micro-papillary carcinoma	4	1.26	+	0.74	4.74	0.19	+
mixed ductolobular adeno-carcinoma + DCIS grade 2	4	1.05	+	0.54	6.67	0.15	+
mixed invasive ductolobular carcinoma + DCIS grade 2	4	0.98	+	0.42	6.46	0.24	+
ILC + LCIS	4	1.07	+	0.60	3.74	0.16	+
mucinous carcinoma	4	1.37	+	1.17	6.55	0.11	+

Table 8.3: Comparison of the diagnostic performance of quantitative DWI following DCE-MRI as problem solver for BI-RADS 3 and 4 lesions. Demonstrated is the diagnostic performance and 95% CI of ADC and IVIM implemented after DCE-MRI as problem solver for lesions classified as BI-RADS 3 and 4. The analysis was performed on all lesions (n = 139). Lesions identified on DCE-MRI as BI-RADS 3 or 4 (n = 26) were additionally evaluated by quantitative DWI. For the remainder of the lesions (n = 113) the endpoint was DCE-MRI. * indicates a significant difference.

	TP	**TN**	**FP**	**FN**	**Se** (%)	**Sp** (%)	**NPV** (%)	
DCE-MRI	116	7	16	0	100 (96.0-100)	30.4 (14.0-53.0)	100 (56.0-100)	
DCE-MRI + ADC	115	8	15	1	99.1 (94.6-100)	34.8 (17.2-57.2)	88.9 (50.7-99.4)	p = 0.5 vs. DCE-MRI
DCE-MRI + IVIM	115	13	10	1	99.1 (94.6-100)	56.5 (34.9-76.1)	92.9 (64.2-99.6)	p = 0.016* vs. DCE-MRI

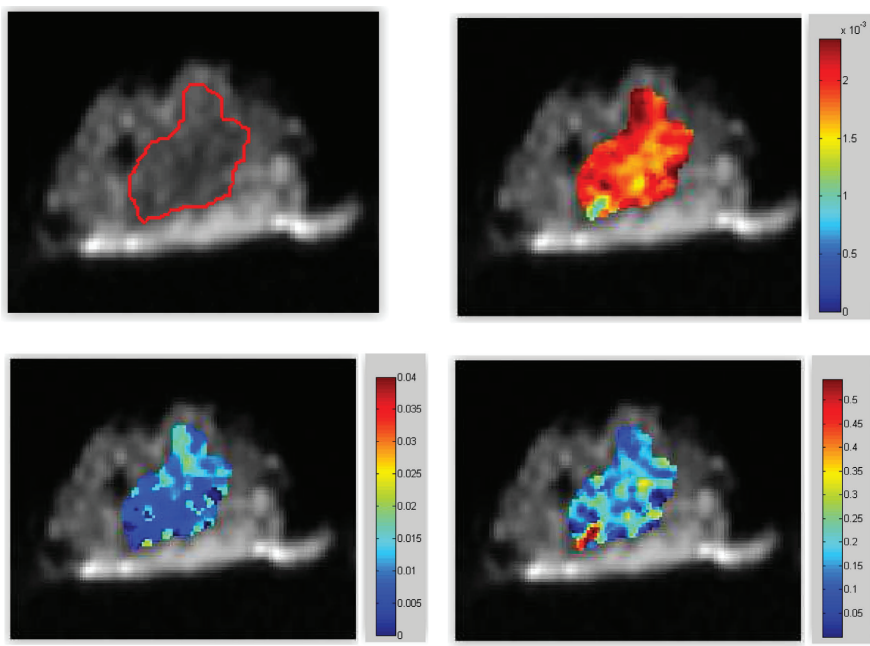

Figure 8.2: Example of adenosis. Voxels were included within a freeform margin around the lesion (top left) and the three IVIM parameters were calculated: molecular diffusion (top right), microperfusion (bottom left) and fraction of microperfusion (bottom right).

8.5 Discussion

The aim of this study was to validate the diagnostic use of quantitative DWI implemented after DCE-MRI in the workup of BI-RADS 3 and 4 breast lesions by implementing a previously validated method for semi-automated breast lesion analysis (*12*). The Se and NPV of DCE-MRI alone in this study were 100% with a Sp of 30.4%, thereby yielding no false negatives, and therefore safe exclusion of malignancy. The NPV of IVIM was 57.1% with a Se and Sp of respectively 92.2% and 52.2%, which is generally too low to allow safe exclusion of malignancy. This means that IVIM may not be able to replace DCE-MRI in the diagnostic workup of breast lesions.

DCE-MRI alone generally results in a negative predictive value of more than 98%, which is confirmed in this study and is enough to safely exclude malignancy (*1–3*). This is mainly based on non-enhancement of breast lesions. However, enhancement patterns of benign and malignant breast lesions can show considerable overlap on DCE-MRI, especially for BI-RADS 3 and 4 lesions which are then mostly scheduled for invasive procedures. To reduce the number of invasive procedures, DCE-MRI followed by quantitative DWI can have potential. The Se and NPV of IVIM or ADC however needs to be sufficient (>98%) to allow for safe exclusion of malignancy.

When IVIM was implemented after DCE-MRI as problem solver for BI-RADS 3 and 4 lesions, the combined Sp of DCE-MRI followed by IVIM increased significantly from 30.4% to 56.5%; this contradicts previous findings on the integration of DCE-MRI and DWI for breast lesion classification, which suggested no benefit of combining DCE-MRI and DWI (*23*). The likely reasons for that are the differences in the approach of optimizing the differentiation between benign and malignant lesions.

The semi-automated method of breast lesion analysis presented in this and previous paper was optimized for excluding breast cancer and preventing biopsies by aiming for a high Se (>98%) with maximal Sp. This approach is inherently different from detecting cancer by optimizing the receiver operating curve and maximizing the area under the curve such that an optimal set of Se and Sp is obtained. DCE-MRI already has a Se and Sp near 100% and 82.5% respectively in non-calcified breast lesions, resulting in a negative predictive value (NPV) higher than 98%, and is thereby able to safely exclude malignancy (*1*, *4*). Therefore for DWI to be implemented successfully along DCE-MRI, the Se should be high (>98%) while the Sp is optimized as high as possible. In the current paper we show that this approach is beneficial for BI-RADS 3 and 4 lesions by proving additional Sp and potentially a reduced number of unnecessary biopsies.

For 11 benign lesions classified as BI-RADS 3 or 4 on DCE-MRI, IVIM was negative

for 6 lesions and the ADC was negative for 1 lesion. However, the combined NPV of DCE-MRI followed by IVIM was too low (92.9%) to allow safe exclusion of malignancy. This indicates that additional optimization of the semi-automated method and possibly a larger group of BI-RADS 3 and 4 lesions are necessary to utilize the gained Sp with sufficient NPV.

For DCE-MRI followed by the ADC, no improvement of the Sp compared to DCE-MRI alone was observed. The ADC can therefore not replace DCE-MRI. These findings are comparable to a previous study investigating whether adding an ADC threshold to DCE-MRI could improve the positive predictive value of breast MRI (*24*). They found a Sp of 47% in combination with 100% Se, however significance was not reached. Also, a study to differentiate between DCIS and invasive breast carcinoma did not find a significant improvement of the diagnostic performance when ADC was compared to DCE-MRI (*25*). A meta-analysis found a Se and Sp of 91.6% and 85.5% respectively (*16*). They optimized their Se and Sp by aiming for the optimum in the receiver-operating curve. Although the Se and Sp of combined DCE-MRI and ADC were higher than either DCE-MRI or ADC alone, this optimization strategy yields a Se which is still too low too safely exclude malignancy.

The diagnostic performance of quantitative DWI depends heavily on the strategy which is used to discriminate benign from malignant lesions using the ADC and IVIM. Some groups raised the Se (93-96%) of the ADC, reducing Sp (55-56%) (*26*, *27*). Others aimed the opposite, reducing Se (52-70%) with high Sp (85-100%) (*10*, *28*, *29*), or simply optimized the receiver-operator curve (86-92%) (*30*, *31*).

In the current study a recently published method was implemented which was designed and validated for excluding cancer by maximizing Sp while maintaining Se near 100% (*12*). This explains the relatively lower Sp presented in this study compared to literature values. However, all Sp of DWI which is gained using this strategy is profitable and can be used to potentially reduce invasive procedures which are indecisive after DCE-MRI by ruling out malignancy, as long as the Se of DWI is high enough. This approach is inherently different to previously published studies that aimed to prove malignancy by increasing the positive predictive value of DWI following DCE-MRI (*24*).

8.5.1 Limitations

A technical limitation in this study is that with the use of additional b-values, especially additional ones in the range between 0 and 50 s/mm^2 and beyond 1000 s/mm^2,

the assessed IVIM parameters might become more robust and potentially yield a higher Sp (*32*). Another limitation is that despite the sizable number of 139 breast lesions included in this prospective study, the demonstration that IVIM analysis of DWI data has additional value for correctly identifying benign BI-RADS 3 and 4 lesions, relies on observations made in 26 lesions only. Also, the study is limited by the retrospective acquisition of the BI-RADS classification from DCE-MRI structured reports. In addition, two malignant BI-RADS 3 lesions were under-classified in retrospect because they had not the typical characteristics of a malignant lesion.

The inclusion criterion of at least 1 cm in diameter, whilst beneficial to the accuracy and reproducibility of the outcomes, limits this study to only a portion of those breast lesions assessable by DCE-MRI. The NPV of the ADC is however reported similar (96%) for small (≤ 1 cm) and large (> 1 cm) lesions (*13*).

Our study included 83.5% malignant lesions, which is comparable to previously published studies (66.7-95.9%) including only lesions of at least 1 cm (*14*, *15*). In addition, our hospital is a center for high risk patients groups (i.e. BRCA) as well as advanced breast cancer. This may explain the relatively high number of malignancies over 1 cm found in our patients, and also the relatively low Sp of DCE-MRI alone. We expect that for this group of complex patients the BI-RADS classification is more frequently over-classified, resulting in more biopsies, to be on the safe side.

8.5.2 Conclusions

In conclusion, this study demonstrates that quantitative DWI has a lower NPV compared to DCE-MRI for evaluation of breast lesions and may therefore not be able to replace DCE-MRI; when implemented after DCE-MRI as problem solver for BI-RADS 3 and 4 lesions the combined specificity improves significantly.

8.6 Acknowledgements

The authors thank MRI system specialist Peter Kappert for acquisition of the data.

8.7 References

(*1*) Dorrius, M. D., Pijnappel, R. M., Sijens, P. E., van der Weide, M. C., and Oudkerk, M. (2012). The negative predictive value of breast Magnetic Resonance Imaging in noncalcified BIRADS 3 lesions. *European Journal of Radiology 81*, 209–213.

(*2*) Gokalp, G., and Topal, U. (2006). MR imaging in probably benign lesions (BI-RADS category 3) of the breast. *European Journal of Radiology 57*, 436–444.

(*3*) Moy, L. et al. (2009). Is breast MRI helpful in the evaluation of inconclusive mammographic findings? *AJR.American journal of roentgenology 193*, 986–993.

(*4*) Strobel, K., Schrading, S., Hansen, N. L., Barabasch, A., and Kuhl, C. K. (2015). Assessment of BI-RADS category 4 lesions detected with screening mammography and screening US: utility of MR imaging. *Radiology 274*, 343–351.

(*5*) Nassar, A. (2011). Core needle biopsy versus fine needle aspiration biopsy in breast–a historical perspective and opportunities in the modern era. *Diagnostic cytopathology 39*, 380–388.

(*6*) Iima, M. et al. (2011). Apparent diffusion coefficient as an MR imaging biomarker of low-risk ductal carcinoma in situ: a pilot study. *Radiology 260*, 364–372.

(*7*) Bihan, D. L., Breton, E., Lallemand, D., Aubin, M. L., Vignaud, J., and Laval-Jeantet, M. (1988). Separation of diffusion and perfusion in intravoxel incoherent motion MR imaging. *Radiology 168*, 497–505.

(*8*) Bickel, H. et al. (2015). Quantitative apparent diffusion coefficient as a noninvasive imaging biomarker for the differentiation of invasive breast cancer and ductal carcinoma in situ. *Investigative radiology 50*, 95–100.

(*9*) Hirano, M., Satake, H., Ishigaki, S., Ikeda, M., Kawai, H., and Naganawa, S. (2012). Diffusion-weighted imaging of breast masses: comparison of diagnostic performance using various apparent diffusion coefficient parameters. *AJR.American journal of roentgenology 198*, 717–722.

(*10*) Cheng, L. et al. (2013). Optimization of apparent diffusion coefficient measured by diffusion-weighted MRI for diagnosis of breast lesions presenting as mass and non-mass-like enhancement. *Tumour biology : the journal of the International Society for Oncodevelopmental Biology and Medicine 34*, 1537–1545.

(*11*) Liu, C., Liang, C., Liu, Z., Zhang, S., and Huang, B. (2013). Intravoxel incoherent motion (IVIM) in evaluation of breast lesions: comparison with conventional DWI. *European Journal of Radiology 82*, e782–9.

(*12*) Dijkstra, H. et al. (2015). Semi-automated quantitative intravoxel incoherent motion analysis and its implementation in breast diffusion-weighted imaging. *Journal of magnetic resonance imaging : JMRI*.

(*13*) Partridge, S. C. et al. (2010). Apparent diffusion coefficient values for discriminating benign and malignant breast MRI lesions: effects of lesion type and size. *AJR.American journal of roentgenology 194*, 1664–1673.

(*14*) Kul, S., Cansu, A., Alhan, E., Dinc, H., Gunes, G., and Reis, A. (2011). Contribution of diffusion-weighted imaging to dynamic contrast-enhanced MRI in the characterization of breast tumors. *AJR.American journal of roentgenology 196*, 210–217.

(*15*) Vignati, A. et al. (2011). Performance of a fully automatic lesion detection system for breast DCE-MRI. *Journal of magnetic resonance imaging : JMRI 34*, 1341–1351.

(*16*) Zhang, L., Tang, M., Min, Z., Lu, J., Lei, X., and Zhang, X. (2015). Accuracy of combined dynamic contrast-enhanced magnetic resonance imaging and diffusion-weighted imaging for breast cancer detection: a meta-analysis. *Acta Radiologica (Stockholm, Sweden : 1987)*.

(*17*) de Almeida, J. R. M., Gomes, A. B., Barros, T. P., Fahel, P. E., and de Seixas Rocha, M. (2015). Subcategorization of Suspicious Breast Lesions (BI-RADS Category 4) According to MRI Criteria: Role of Dynamic Contrast-Enhanced and Diffusion-Weighted Imaging. *AJR.American journal of roentgenology 205*, 222–231.

(*18*) Pinker, K. et al. (2014). Improved diagnostic accuracy with multiparametric magnetic resonance imaging of the breast using dynamic contrast-enhanced magnetic resonance imaging, diffusion-weighted imaging, and 3-dimensional proton magnetic resonance spectroscopic imaging. *Investigative radiology 49*, 421–430.

(*19*) Bihan, D. L., Turner, R., Moonen, C. T., and Pekar, J. (1991). Imaging of diffusion and microcirculation with gradient sensitization: design, strategy, and significance. *Journal of magnetic resonance imaging : JMRI 1*, 7–28.

(*20*) Muller, M. F., Prasad, P., Siewert, B., Nissenbaum, M. A., Raptopoulos, V., and Edelman, R. R. (1994). Abdominal diffusion mapping with use of a whole-body echo-planar system. *Radiology 190*, 475–478.

(*21*) Turner, R., Bihan, D. L., Maier, J., Vavrek, R., Hedges, L. K., and Pekar, J. (1990). Echo-planar imaging of intravoxel incoherent motion. *Radiology 177*, 407–414.

(*22*) Newcombe, R. G. (1998). Two-sided confidence intervals for the single proportion: comparison of seven methods. *Statistics in medicine 17*, 857–872.

(*23*) Fusco, R. et al. (2015). Integration of DCE-MRI and DW-MRI Quantitative Parameters for Breast Lesion Classification. *BioMed research international 2015*, 237863.

(*24*) Partridge, S. C., DeMartini, W. B., Kurland, B. F., Eby, P. R., White, S. W., and Lehman, C. D. (2009). Quantitative diffusion-weighted imaging as an adjunct to conventional breast MRI for improved positive predictive value. *AJR.American journal of roentgenology 193*, 1716–1722.

(*25*) Wang, Y. et al. (2015). Diffusion-tensor imaging as an adjunct to dynamic contrast-enhanced MRI for improved accuracy of differential diagnosis between breast ductal carcinoma in situ and invasive breast carcinoma. *Chinese journal of cancer research = Chung-kuo yen cheng yen chiu 27*, 209–217.

(*26*) Partridge, S. C., Demartini, W. B., Kurland, B. F., Eby, P. R., White, S. W., and Lehman, C. D. (2010). Differential diagnosis of mammographically and clinically occult breast lesions on diffusion-weighted MRI. *Journal of magnetic resonance imaging : JMRI 31*, 562–570.

(*27*) Ochi, M. et al. (2013). Diffusion-weighted imaging (b value = 1500 s/mm(2)) is useful to decrease false-positive breast cancer cases due to fibrocystic changes. *Breast cancer (Tokyo, Japan) 20*, 137–144.

(*28*) Stadlbauer, A. et al. (2009). Diffusion-weighted MR imaging with background body signal suppression (DWIBS) for the diagnosis of malignant and benign breast lesions. *European radiology 19*, 2349–2356.

(*29*) Sahin, C., and Aribal, E. (2013). The role of apparent diffusion coefficient values in the differential diagnosis of breast lesions in diffusion-weighted MRI. *Diagnostic and interventional radiology (Ankara, Turkey) 19*, 457–462.

(*30*) Pereira, F. P. et al. (2009). Assessment of breast lesions with diffusion-weighted MRI: comparing the use of different b values. *AJR.American journal of roentgenology 193*, 1030–1035.

(*31*) Rubesova, E., Grell, A. S., Maertelaer, V. D., Metens, T., Chao, S. L., and Lemort, M. (2006). Quantitative diffusion imaging in breast cancer: a clinical prospective study. *Journal of magnetic resonance imaging : JMRI 24*, 319–324.

(*32*) Peters, N. H., Vincken, K. L., van den Bosch, M. A., Luijten, P. R., Mali, W. P., and Bartels, L. W. (2010). Quantitative diffusion weighted imaging for differentiation of benign and malignant breast lesions: the influence of the choice of b-values. *Journal of magnetic resonance imaging : JMRI 31*, 1100–1105.